

ARTICLE TYPE

The Secret Lives of Open Clusters: a Multiwavelength Examination of Three Open Clusters

Kristen C. Dage,¹ Emily L. Hunt,² Jasmine Anderson-Baldwin,⁴ Evangelia Tremou,⁶ Khushboo K. Rao,⁷ Kwangmin Oh,⁸ Malu Sudha,⁹ Jarrod Hurley,⁴ Robert D. Mathieu,¹⁰ Aarya Patil,¹¹ Richard M. Plotkin,¹² Andrew M. Hopkins,¹⁴ Jacco Th. van Loon,¹⁵ and Jayde Willingham¹⁴

¹International Centre for Radio Astronomy Research — Curtin University, GPO Box U1987, Perth, WA 6845, Australia

²Department of Astrophysics, University of Vienna, Türkenschanzstrasse 17, 1180 Wien, Austria

³Max-Planck-Institut für Astronomie, Königstuhl 17, 69117 Heidelberg, Germany

⁴Centre for Astrophysics and Supercomputing, Swinburne University of Technology, Hawthorn, VIC 3122, Australia

⁵ARC Centre of Excellence for Gravitational Wave Discovery (OzGrav), Hawthorn, VIC 3122, Australia

⁶National Radio Astronomy Observatory, Socorro, NM 87801, USA

⁷Institute of Astronomy, National Central University, Taiwan

⁸Center for Data Intensive and Time Domain Astronomy, Department of Physics and Astronomy, Michigan State University, East Lansing, MI 48824, USA

⁹Department of Physics & Astronomy, Wayne State University, 666 W. Hancock St, Detroit, MI 48201, USA

¹⁰Department of Astronomy, University of Wisconsin - Madison, Madison WI, USA

¹¹Max-Planck-Institut für Astronomie, Königstuhl 17, D-69117 Heidelberg, Germany

¹²Department of Physics, University of Nevada, Reno, NV 89557, USA

¹³Nevada Center for Astrophysics, University of Nevada, Las Vegas, NV 89154, USA

¹⁴School of Mathematical and Physical Sciences, 12 Wally's Walk, Macquarie University, NSW 2109, Australia

¹⁵Lennard-Jones Laboratories, Keele University, ST5 5BG, UK

Abstract

Star clusters are well known for their dynamical interactions, an outcome of their high stellar densities; in this paper we use multiwavelength observations to search for the unique outcomes of these interactions in three nearby Galactic open clusters: IC 2602 (30 Myr), NGC 2632 (750 Myr) and M67 (4 Gyr). We compared X-ray observations from all-sky surveys like eROSITA, plus archival observations from *Chandra* X-ray Observatory, survey radio observations from ASKAP's Evolutionary Map of the Universe survey plus archival VLA observations, in conjunction with new cluster catalogs with Gaia. From X-ray, we found 77 X-ray sources likely associated with IC 2602, 31 X-ray sources in NGC 2632, and 31 near M67's central regions. We were further able to classify these X-ray sources based on their optical variability and any radio emission. Three IC 2602 X-ray sources had radio counterparts, which are likely all chromospherically active binary stars. We also identified luminous radio and X-ray variability from a spectroscopic triple system in M67, WOCS 3012/S1077, which is either consistent with a quiescent black hole binary, or due to an active binary stellar system. A recent population study of optical variables by Anderson & Hunt 2025 shows that the population of optical variables in open clusters clearly changes over cluster age; this pilot study gives evidence that the X-ray population also changes with time, and demonstrates the need for a broader multiwavelength study of Galactic open clusters.

1. Introduction

Open clusters (OCs) are densely bound collections of stars, born out of the collapse of large clouds of gas. They can range in age from a few tens of Myr to a few Gyr, and are single stellar populations (SSPs Portegies Zwart et al., 2010; Cantat-Gaudin & Casamiquela, 2024). Due to this, they are useful as tracers of Galactic chemical trends (Donor et al., 2020), as well as understanding simple stellar evolution in a dynamical environment (Hurley et al., 2005; Hunt & Reffert, 2024). Because of their distribution in the Milky Way and proximity to Earth, their individual stars can be resolved and well-studied.

Data from ESA's Gaia satellite (Gaia Collaboration et al., 2016) has completely revolutionized the census of OCs in just a few short years (Cantat-Gaudin & Casamiquela, 2024). Since the release of Gaia DR2 (Gaia Collaboration et al., 2018), thousands of new OCs have been discovered (e.g. Castro-Ginard et al., 2018; Liu & Pang, 2019; Hunt & Reffert, 2023), over a thousand OCs from before Gaia have been ruled out as asterisms (Cantat-Gaudin et al., 2020; Hunt & Reffert, 2023),

and the general quality of the OC census has improved, both in terms of improved membership determination (Cantat-Gaudin et al., 2018; Dias et al., 2021; Hunt & Reffert, 2023; Perren et al., 2023) and improved determination of parameters such as cluster distance, age, and mass (Cantat-Gaudin et al., 2020; Hunt & Reffert, 2023; Cavallo et al., 2024a). There has hence never been a better time to do science with OCs in the Milky Way.

With the available wealth of X-ray and radio surveys, it is now possible to delve into the contents of OCs by searching for their multiwavelength counterparts. For example, Belloni et al. (1998); van den Berg et al. (2004) and Mooley & Singh (2015) used X-ray observations from *Chandra* and XMM-Newton to identify X-ray counterparts to individual cluster members of the old open cluster M67. Radio emission is also helpful to classify X-ray sources (e.g., Driessen et al., 2024; Paduano et al., 2024, among others)

Two major sources of uncertainty for these kinds of studies are 1) determining whether a given X-ray point source has an optical counterpart (which is dependent on positional

accuracy), and 2) whether that optical counterpart is a cluster member. While the association of multiwavelength sources to OC members is challenging, it is useful to find unique sources to benchmark SSP evolution in a dense field.

In old open clusters (older than a few Gyr), most single stars have spun down due to magnetic braking and are consequently faint in X-ray (e.g. Caillault, 1996). In clusters around this age, bright X-ray sources are instead dominated by binaries. In binaries with relatively short separations (or relatively large radii), tidal interactions can force the stars into a higher rotation rate, leading to higher X-ray emission (e.g. Belloni et al., 1998). In other cases, accretion onto compact objects within a binary also produces luminous X-ray sources. Multiwavelength observations, particularly in the X-ray, allow us to probe the populations of these close binary systems. Since binary populations are drivers of cluster evolution (Hut et al., 1992), this in turn gives us greater understanding of the dynamical evolution of clusters.

Beyond the influence that dynamics provide to enhance BH formation in clusters, from the observational standpoint, it is natural to associate the origins of many black holes with star clusters, including new evidence in the form of Gaia BH3 (Gaia Collaboration et al., 2024), which is found in the stellar stream of ED-2, a disrupted low mass cluster (Balbinot et al., 2024). In this paper, we use archival and survey observations from X-ray and radio facilities to search for multiwavelength counterparts to individual OC stars, as identified by Hunt & Reffert (2024). We specifically target nearby OCs from three different ages, and compare their unique multiwavelength contents, with the aim to use this information to provide a benchmark for the contents of open clusters of different ages and masses to improve future iterations of N-body simulations of open clusters.

2. Data and Analysis

For our cluster sample, we use individual cluster members as identified in data from Gaia DR3 (Gaia Collaboration et al., 2023) by Hunt & Reffert (2024). We search for X-ray counterparts from *Chandra* (Weisskopf et al., 2002), *XMM-Newton* (Jansen et al., 2001), *eROSITA* (Merloni et al., 2024), as well as radio counterparts from the Evolutionary Map of the Universe (EMU) survey (Hopkins et al., 2025) and the Karl G. Jansky Very Large Array (Perley et al., 2011). We also take advantage of the Gaia variability flags to further classify sources, and we search for evidence of optical variability and further classification thanks to work by Eyer et al. (2023).

2.1 Cluster sample

The cluster sample is selected as follows; we targeted nearby OCs (within 1 kpc) observed in X-ray, targeting three different age ranges; a young OC, IC 2602 (30 Myr), a middle age OC, NGC 2632 (350 Myr), and an old cluster, NGC 2682/M67 (4 Gyr). IC 2602 and NGC 2632 are both within the publicly-released German *eROSITA* footprint, and M67 has been well studied in X-ray with *ROSAT*, *Chandra* and *XMM-Newton* (Belloni et al., 1998; van den Berg et al., 2004;

Mooley & Singh, 2015). M67 is one of the most well studied open clusters in almost every wavelength (except radio), with optical studies to determine stellar cluster membership, and ultraviolet studies to find evidence of a blue straggler population (Peterson et al., 1984).

Blue stragglers are bluer and brighter than the main sequence turnoff stars (Sandage, 1953). Stellar merger, collision, and mass-transfer are known to be the primary channels for their formation (Boffin et al., 2015). Due to the low density of open clusters, stellar merger and mass-transfer are the only viable channels. The formation of blue stragglers due to multiple stellar interactions places them among the massive populations in star clusters (Shara et al., 1997), and therefore they are representatives of dynamical ages of their host clusters as well (Ferraro et al., 2012; Rao et al., 2023)

We revisit M67 in light of new Gaia memberships. For our multi-wavelength study of M67, we can take advantage of Geller et al. (2015)'s spectroscopic study of M67 members to search for radial velocity variability. We report the cluster properties in Table 1.

2.2 X-ray

Due to their extended size (often spanning several degrees), nearby OCs are often not the target of detailed X-ray studies (with the exception of M67, which has been well studied at the center), but benefit from sensitive all-sky X-ray surveys like *eROSITA*, which can provide a consistent picture of the entire cluster. For IC 2602 and NGC 2632, we searched for X-ray counterparts to individual cluster members in *eROSITA*. We rejected three matches in IC 2602 because the optical magnitude was brighter than 6, and the X-rays were likely due to optical loading (for further discussion, see Merloni et al., 2024; Saeedi et al., 2022).

M67 is nominally in the publicly available *eROSITA* footprint. However, we did not identify any X-ray counterparts from *eROSITA*. We therefore made use of archival pointed observations from *Chandra* and *XMM-Newton*. For *Chandra*, we used the *Chandra* Source Catalog version 2.1 (Evans et al., 2010), which contains two relevant observations: ObsID 1873 (50 ks, 2001 May 31, PI: Belloni) and ObsID 17020 (10 ks, 2015 February 26, PI: van den Berg). For *XMM-Newton*, we examined the European Photon Imaging Camera (EPIC) Pipeline Processed Source (PPS) catalogs for ObsID 0212080601 (15 ks, 2005 May 8, PI: Jansen) and ObsID 0109461001 (10 ks, 2001 October 20, PI: Mason).

We were particularly interested in follow up on a specific X-ray source in M67, WOCS 3012/S1077. We extracted it from the merged *Chandra* dataset and estimated its unabsorbed fluxes using the *srcflux* script in *CIAO*. A power-law spectral model with a fixed photon index of $\Gamma = 2$ was adopted, and the hydrogen column density was fixed at $N_H = 2.2 \times 10^{20} \text{ cm}^{-2}$ (van den Berg et al., 2004).

For ObsID 1873 (effective exposure 46.26 ks), the unabsorbed flux in the 0.5–8.0 keV band was $7.8_{-0.49}^{+0.49} \times 10^{-14} \text{ erg cm}^{-2} \text{ s}^{-1}$. For the same model, the fluxes in the 1–10 keV and 0.5–10 keV bands were $4.75_{-0.40}^{+0.40} \times 10^{-14}$ and $7.87_{-0.49}^{+0.50} \times 10^{-14} \text{ erg cm}^{-2} \text{ s}^{-1}$,

Table 1. Observed cluster properties from Hunt & Reffert (2024), except for the age of M67, as the ages are underestimated for clusters with blue straggler stars (Hunt & Reffert, 2024; Cavallo et al., 2024b). M67 is estimated to be around 4 Gyr old (Reyes et al., 2024, and references therein).

Cluster Name	RA	Dec	Age (Gyr)	Dist (pc)	r_f (deg)	Mass (M_\odot)
IC 2602	160.97308272	-64.39323626	0.03	150.6	3.24	344 ± 42
NGC 2632	130.08810396	+19.66587324	0.75	183.5	4.28	1012 ± 74
NGC 2682/M67	132.84984192	+11.81745461	4	837.3	1.41	2761 ± 403

Table 2. Variability flags and optical periods for X-ray sources in IC 2602, where reported in Eyer et al. (2023). Less than half of these X-ray sources have detected variability.

Gaia ID	class name	period
5237279792173016832	RS	-
5239251727594949120	SOLAR_LIKE	-
5239525196750143616	RS	-
5239701569617071872	YSO	-
5239758155778687360	RS	-
5239851962193200896	SOLAR_LIKE	-
5241082315708039168	YSO	-
5241621385657305856	YSO	-
5239242660940082432	COMP_VAR_VSX_2019	1.19
5239723525484923904	COMP_VAR_VSX_2019	-
5251802519709841280	COMP_VAR_VSX_2019	-
5239746271633131904	ASASSN_VAR_JAYASINGHE_2019	2.00
5242010093028921856	COMP_VAR_VSX_2019	-
5251805715165696384	ASASSN_VAR_JAYASINGHE_2019	0.21
5239758155778687360	COMP_VAR_VSX_2019	-
5241350287303624832	COMP_VAR_VSX_2019	-
5239498744077038976	ASASSN_VAR_JAYASINGHE_2019	0.62
5244883529229180928	ASASSN_VAR_JAYASINGHE_2019	1.83
5239401432972879872	COMP_VAR_VSX_2019	5.93
5239626420542800512	ASASSN_VAR_JAYASINGHE_2019 (RS)	0.99

Table 3. Gaia variability flags and optical periods for X-ray sources in NGC 2632 (where available) from Eyer et al. (2023). The majority of the X-ray sources in NGC 2632 are from rotational variables.

Gaia ID	class name	period
661190015991474688,	ECL	-
660225916090501376	GAIA_ROT_GAIA_2017	5.85
661190153430426880	RS	9.76
664453778817920256	ASASSN_VAR_JAYASINGHE_2019	-
661458365546507776	SOLAR_LIKE	8.90
661311752544249088,	GAIA_ROT_GAIA_2017	2.99
661408818803811200	SOLAR_LIKE	12.22
661216743570426240	GAIA_ROT_GAIA_2017	3.23
664288577196528128	SB9_SB_POURBAIX_2004	5.97
661268940310277888	GAIA_ROT_GAIA_2017	4.14
661289105178505344	SB9_SB_POURBAIX_2004	45.98
661271173693364864	COMP_VAR_VSX_2019	-
661306319407420160	GAIA_ROT_GAIA_2017	6.04
663140171661012480	KEPLERGAIA_BY_ROT_DISTEFANO_2023	1.56
659645030354241536	GAIA_ROT_GAIA_2017	11.29
661294332158553856	GAIA_ROT_GAIA_2017	7.14
664436770747504128	GAIA_ROT_GAIA_2017	12.78
660998975844267264	SOLAR_LIKE	9.12
661419264165477504	GAIA_ROT_GAIA_2017	2.59
665129291274749696	GAIA_ROT_GAIA_2017	9.50
664324684984105728	SB9_SB_POURBAIX_2004	13.28
660939258619177984	GAIA_ROT_GAIA_2017	12.62
661148268907314432	SOLAR_LIKE	4.53
661396754238802816	HIP_VAR_ESA_1997	-
664478620908806784	SOLAR_LIKE -	
664710686582129536	SOLAR_LIKE	

Table 4. Variability flags and optical periods compiled by Eyer et al. (2023) along with binary membership from Geller et al. (2015) for M67 X-ray sources. (BL)M stands for likely binary member, BM for binary member, SM for single member, (BL)N for **binary likely non-members, and U for unknown**.

GAIA_ID	Mm	class name	period
604906771677660544	(BL)M	CATALINA_VAR_DRAKE_2014 (ECL)	0.51
604911307163200000	BN	COMP_VAR_VSX_2019	-
604911509025877248	(BL)M	ATLAS_VAR_HEINZE_2018 (DSCT GDOR SXPHE)	0.36
604914983655019520	BM	LAMOST_RAD_VEL_VAR_TIAN_2020	-
604916422468464768	BM	SB9_SB_POURBAIX_2004	4.36
604916559907415040	BM	SB9_SB_POURBAIX_2004	31.78
604917285757663872	BM		
604917354477131392	BM	SOLAR_LIKE	
604917491916095872	BM	SB9_SB_POURBAIX_2004(RS)	10.06
604917526275831040	BM		
604917629355039360	BM	COMP_VAR_VSX_2019	-
604917629355038848	BM	SB9_SB_POURBAIX_2004	7.16
604917663714774784	SM		
604917728138508160	BM	SB9_SB_POURBAIX_2004	42.83
604917934296938240	BM	SB9_SB_POURBAIX_2004	11.02
604918041671889792	(BL)M	ASASSN_VAR_JAYASINGHE_2019 (ECL)	0.44
604918179110923392	SM		
604918213470564992	(BL)M	CATALINA_VAR_DRAKE_2014 (ECL)	0.36
604920683076006272	BM	SB9_SB_POURBAIX_2004	7.65
604920756091231488	(BL)M	SOLAR_LIKE	
604920824810533632	(BL)N	RS	
604921030968952832	BM	SB9_SB_POURBAIX_2004 (RS)	18.39
604921374566324992	BM	COMP_VAR_VSX_2019	2.6
604921374566321920	BM	SB9_SB_POURBAIX_2004	1495.0
604921855602675968	BM	COMP_VAR_VSX_2019	1.44
604923947251366656	U	LINEAR_VAR_PALAVERSA_2013 (RS)	0.27
604969787437702784	U	SOLAR_LIKE	0.26

respectively. Assuming a distance of 820 pc to M67 (van den Berg et al., 2004), this flux corresponds to an X-ray luminosity of $L_X \approx 6.3 \times 10^{30}$ erg s $^{-1}$ in the energy band of 0.5–8.0 keV.

In contrast, no significant X-ray emission was detected at the same coordinates in ObsID 17020 (effective exposure 9.82 ks). Using the Bayesian prescription for Poisson statistics in the case of zero source counts (Kraft et al., 1991), we derived a 90% confidence count-rate upper limit of 2.34×10^{-4} counts s $^{-1}$. Assuming the same spectral model as above ($\Gamma = 2$, $N_H = 2.2 \times 10^{20}$ cm $^{-2}$), the corresponding unabsorbed flux upper limits are 9.4×10^{-16} erg cm $^{-2}$ s $^{-1}$ (0.5–10 keV) and 8.2×10^{-16} erg cm $^{-2}$ s $^{-1}$ (1–10 keV), which translate to luminosity limits of $L_X < 7.6 \times 10^{28}$ erg s $^{-1}$ and $L_X < 6.6 \times 10^{28}$ erg s $^{-1}$, respectively.

2.3 Radio

IC 2602 has been observed by the *Australian SKA Pathfinder Telescope* EMU survey (Hopkins et al., 2025). We searched for radio counterparts to X-ray point sources associated with cluster stars in the pipeline-processed catalogs. The EMU survey will mainly be sensitive to background AGN, but at the 150 pc distance of IC 2602, it is also sensitive to radio emission produced by chromospherically active contact binaries.

Of the 77 X-ray sources with high probability matches to cluster stars, only three had detected radio counterparts in EMU, all in the central region of IC 2602.

NGC 2632 and M67 are too far north to be observed by ASKAP. However, M67 has been observed by VLA on December 11, 2010 (Project code: VLA/10B-173) for four hours in total. The observations were taken with the C-band receiver (centered at 5 GHz) with a 2 GHz total bandwidth. 3C286 (J1331+3030) was observed and used for bandpass and flux scale calibration and J0842+1835 for gain calibration. The data were calibrated and imaged with CASA (CASA Team et al., 2022). The VLA Pipeline 2024.1.1 (CASA 6.6.1)^a was used to perform flagging and calibration. Briggs weighting with robustness parameter 0 was used to image the data.

We used pyBDSF (Mohan & Rafferty, 2015), to detect radio point sources down to a $\sim 5\sigma$ threshold, and detected 50 unique point sources. We crossmatched VLA and Gaia data for potential matches within 1'', and found four radio sources with a Gaia counterpart. Only one of these sources has cluster membership in M67 (604921855602675968, with a flux density of $96 \pm 5\mu\text{Jy}$). One is classified as a background AGN SDSS J085150.31+114855.9 (Gaia DR3 604918380973692800). Two have stellar classifications, Gaia DR3 604918174820102400 is classified as rotating variable EY Cnc, Gaia DR3 604915808290404480 is classified as a cluster member by Fan et al. (1996), but the X-ray counterpart from van den Berg et al. (2004) is classified as a QSO, highlighting the prevalence of background AGN contamination in pre-Gaia cluster catalogs.

2.4 Crossmatching with NWAY

We use NWAY^b (Salvato et al., 2018) to crossmatch between X-ray data from eROSITA and *Chandra* and Gaia fields of IC 2602 and NGC 2632 (querying the full Gaia catalog from the position and Jacobi radius given in Hunt & Reffert 2024).

NWAY computes the match probability, useful in the case of multiple potential matches, and rules out sources with a high probability of chance superposition. Because these open clusters are not very crowded fields, we did not find any issues with crowding or multiple optical counterparts to an X-ray counterpart. NWAY's match probability for all matches was very high (> 95% in all cases).

We crossmatched up to a radius of 5'' for the following reasons: while the positional errors of eROSITA sources typically ranged from 1'' up to 15'', we do not report matches with separations larger than 5''. We shifted the RA and Dec of one catalog in several directions by 10'' and, after rematching, found that the shifted catalogs gave a large number of matches beyond 5'', suggesting that matches with a separation higher than 5'' were contaminated.

For M67, thanks to *Chandra*'s subarcsecond spatial resolution, we considered matches between Gaia and the CSC up to 1''. We only found two XMM-Newton matches to M67 stellar members that were not also detected by *Chandra*. We note that we expect to have different results to Belloni et al. (1998); van den Berg et al. (2004) and Mooley & Singh (2015), as Hunt & Reffert (2024)'s Gaia cluster catalogs are more accurate than those used in previous X-ray studies of M67.

2.5 Optical Variability

We searched for evidence of optical variability using the Gaia variability flags, and Eyer et al. (2023) which crossmatches Gaia data to all known optical surveys. For each cluster, we search the optical counterpart to a given X-ray source in these databases, and we catalog their classification and period if one exists in the literature. A preview of these tables can be seen in the Appendix.

Gaia classifications include solar-like variability, eclipsing binaries, RS Canum Venaticorum, α^2 CVn and associated stars, δ Scuti/ γ Doradus/SX Phoenicis, young stellar objects, RR Lyrae and slowly pulsating B stars. Thanks to longterm optical surveys such as Drake et al. (2014); Watson et al. (2006); Heinze et al. (2018); Tian et al. (2020); Pourbaix et al. (2004); Jayasinghe et al. (2019); Palaversa et al. (2013); Perryman et al. (1997) in some cases, we are able to obtain optical periods for the systems. For the X-ray sources, we report variability class and period (if known) in Tables 2, 3, and 4.

Of the 33 X-ray sources we found associated with a M67 individual star, 27 were found in the Geller et al. (2015) spectroscopic study. Of these, 80% fall in the binary member category, or likely binary member category. Three are likely single members, and two are unknown (but still proper motion members). We report the Geller et al. (2015) binary member

^a<https://science.nrao.edu/facilities/vla/data-processing/pipeline>

^b<https://github.com/JohannesBuchner/nway>

Table 5. IC 2602 cluster members with X-ray from eROSITA and radio from the EMU survey.

GAIA_ID	G_mag	X-ray Flux erg/s (0.2-2.3 keV)	Radio Flux Density mJy (943.5 MHz)
5253546997989686912	10.32	$6.7 \times 10^{-13} \pm 4.7 \times 10^{-14}$	0.18 ± 0.08
5251888522138694656	11.25	$5.0 \times 10^{-13} \pm 4.1 \times 10^{-14}$	0.21 ± 0.02
5239674700295136000	12.23	$1.6 \times 10^{-13} \pm 2.2 \times 10^{-14}$	0.14 ± 0.03

category in Table 4, along with the variability classification from Gaia for M67.

3. Results and Discussion

We used new and archival multiwavelength observations to search the contents of three open clusters: IC 2602 (0.03 Gyr), NGC 2632 (0.35 Gyr) and M67 (4 Gyr).

3.1 IC 2602

Of the 77 X-ray sources associated with IC 2602, only 14 had variability classification or measured periods. Three sources had radio from EMU associated with them, and the radio and X-ray fluxes suggest these systems are chromospherically active binary stars, consistent with Guedel et al. 1995; Driessen et al. 2024 (see also Paduano et al. 2024). The radio and X-ray fluxes of these sources are summarized in Table 5. Other classification of the X-ray sources include young stellar objects, RS Canum Venaticorum, and solar-like sources. Several other of the X-ray sources are unclassified variable sources found in AAVSO and ASAS-SN. The location of these sources on the color-magnitude diagram (CMD) can be seen in Figure 1, and the X-ray luminosity versus optical magnitude in Figure 2. The radio detections appear to be early to mid-F spectral type stars. Based on the CMD of IC 2602, these stars have masses between 1.2 and 1.5 solar masses, which indicates that they have begun to develop convective envelopes, signifying that their stellar structure is changing.

An upper main-sequence star with Gaia ID = 5239843200460432 is identified as a very fast rotator and has also been classified as an SPB variable. This matched to a detection in eROSITA, which we rejected as contaminated as it fell into the optical loading range. If this source is indeed X-ray bright, the combination of SPB variability, rapid rotation, and strong X-ray emission would point toward either the presence of a companion or a Be/Bp spectral classification. Be stars are a subset of B-type stars that host decretion disks driven by their rapid rotation, and a fraction of them are known to exhibit SPB-type pulsations (Rivinius et al., 2016; Shi et al., 2023). Additionally, two other stars, Gaia IDs = 5299121205191777792 and 5239841340702856960, show high RUWE values, strongly suggesting the presence of gravitational companions. Notably, Gaia ID = 5299121205191777792 is even listed in SIMBAD as a double or multiple system.

3.2 NGC 2632

We identified 31 eROSITA sources which can be associated with NGC 2632 stellar members. Of these, 19 showed optical

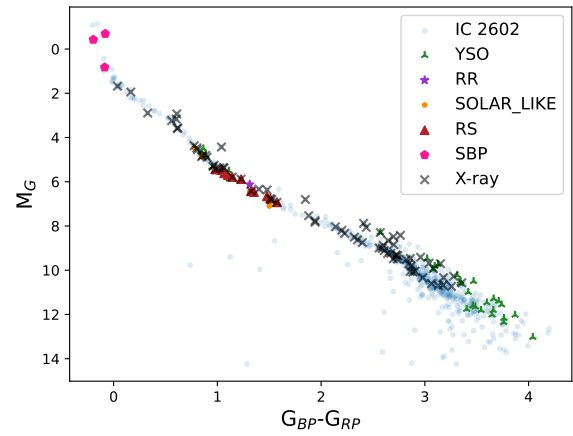


Figure 1. CMD for IC 2602. Black x's are X-rays from eROSITA, green triangles are δ Scuti/ γ Doradus/SX Pheonicis, purple pentagons are ACV systems, red triangles are RS Canum Venaticorum, teal squares are eclipsing binaries and orange points are solar-like variability.

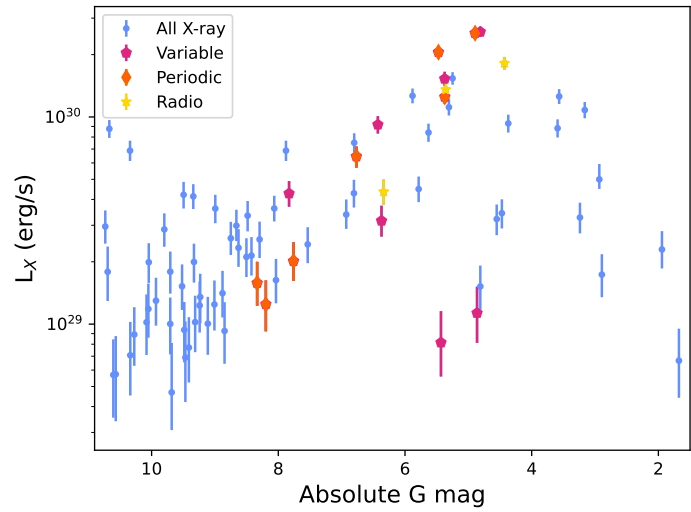


Figure 2. X-ray luminosity (eROSITA band) versus absolute G magnitude for X-ray sources in IC 2602. Sources with variability flags from Eyer et al. (2023) are labeled in orange pentagons, with periodic sources marked with pink diamonds. Three sources (yellow triangles) had radio emission associated with them, but were not flagged as variable by Eyer et al. (2023).

Table 6. Gaia variability flags (Eyer et al., 2023) for stellar members of the three clusters: solar-like variability (SOLAR_LIKE), eclipsing binaries (ECL), RS Canum Venaticorum (RS), α^2 CVn and associated stars (ACV), δ Scuti/ γ Doradus/SX Phoenicis stars (DSCT), young stellar objects (YSO), RR Lyrae (RR), and slowly pulsating B star (SPB). The main types of variability are either due to rotation (ACV, RS, SOLAR_LIKE) or pulsation (DSCT, RR, SPB).

Cluster Name	SOLAR_LIKE	ECL	RS	ACV	DSCT	YSO	RR	SPB
IC 2602	5	-	11	-	-	32	1	3
NGC 2632	155	1	1	2	1	-	-	-
NGC 2682/M67	21	3	8	0	1	-	-	-

variability. The majority of the X-ray systems have solar-like variability, with one eclipsing binary, one RS Canum Venaticorum, rotational sources, and other variability (Pourbaix et al., 2004; Jayasinghe et al., 2019; Perryman et al., 1997; Distefano et al., 2023). The location of the X-ray sources and optical variables on the CMD can be seen in Figure 3, and we plot the X-ray luminosity versus optical magnitude in Figure 4. We searched the VLASS all sky catalog (Lacy et al., 2020), but there were no detected radio counterparts matching to eROSITA cluster associated X-ray sources within $10''$.

One of the upper main-sequence X-ray sources in NGC 2632 (Gaia ID = 664314759317023360, $G = 8.632$ mag, corresponding to an absolute G mag of 2.31) has a $v_{\text{broad}} = 195.29 \pm 2.43 \text{ km s}^{-1}$ and a high RUWE value of 5.12, suggesting the presence of a gravitationally bound companion. The observed X-ray emission may either arise from interaction processes within the system that is also driving rapid stellar rotation, or from a low-mass companion.

3.3 M67

In M67, we found 31 *Chandra* sources associated with an individual cluster member; we plot these sources and the optical variables on M67's CMD in Figure 5, and the X-ray luminosity vs optical magnitude in Figure 6.

We note that our X-ray associations to M67 are significantly different from previous studies (van den Berg et al., 2004; Mooley & Singh, 2015), because despite using the same X-ray observations, our cluster catalog is significantly different. In particular, Belloni et al. (1998)'s ROSAT study, which uses a very different ground-based cluster catalog (where the typical uncertainties are on the order of Gaia at 21st magnitude (~ 1 mas / yr), which is the limiting mag of Gaia). We do not attempt to replicate this particular study because the ROSAT positional uncertainty is significant (ranging from $3''$ to $29''$), and although M67 as an open cluster is less crowded than a globular cluster, that positional uncertainty is still large enough that there can be multiple optical counterparts to a given X-ray source. Using Belloni et al. (1998)'s positions and uncertainties, we found that the only ROSAT sources with relatively small positional uncertainties, which crossmatched to an individual Gaia cluster member, were also found with the *Chandra* data.

In M67, two X-ray sources that are brighter and bluer than the main sequence turnoff are blue stragglers, two X-ray sources located above sub-giant branch stars are evolved BSS/yellow stragglers, and one X-ray source located below the sub-giant branch is a sub-subgiant star (GaiaDR3 ID

604921030968952832). Geller et al. (2017) found two M67 sources as sub-subgiant stars, GaiaDR3 ID 604921030968952832 (S1063), GaiaDR3 ID 604972089540120832 (S1113), and both of those show X-ray emission and are binaries.

Unlike IC 2602 and NGC 2632, where the X-ray studies are complete (if not contaminated due to eROSITA positional uncertainties), the *Chandra* and XMM pointings only targeted near the center of the cluster, and thus our knowledge of M67's contents is less complete.

For the X-ray sources associated with Hunt & Reffert (2024)'s M67 catalog, 27 have been studied spectroscopically by Geller et al. (2015). 21 of these have binary membership classification. Many of these systems are variable, with Gaia variability flags solar-like, ECL, DSCT, RS, and have periods reported in the literature. We note that only 6 of the M67 X-ray sources do not have binary membership (Table 4).

From the VLA observation pointed at M67's center, we identified 50 radio point sources. Of these, only four matched to X-ray and optical sources detected by *Chandra* and the complete Gaia catalog of the central region of M67. Two were classified as QSO/AGN, and were previously classified as M67 candidate members by Fan et al. (1996). Gaia DR3 604918174820102400 is not classified as a cluster member by Hunt & Reffert (2024), and is too faint to have parallax and proper motions measured, but has an 8.4 day optical period. This optical period may be more consistent with a non-member star than an AGN.

Gaia DR3 604921855602675968 (WOCS 3012/S1077) is a cluster member, both from Gaia proper motions (Hunt & Reffert, 2024), but also confirmed via spectroscopy (Geller et al., 2015). The 10GHz radio luminosity of this source, assuming the distance to M67, is $3.96 \pm 0.25 \times 10^{26} \text{ erg/s}$. We analyzed the radio and X-ray luminosities, comparing them to both chromospherically active binary stars (Guedel et al., 1995), (Figure 7) as well as quiescent black hole binaries in Figure 8. In Figure 7, we see that WOCS 3012/S1077 falls in the scatter of the luminous end of the Guedel et al. (1995) relationship for chromospherically active binaries (and on the flatter part of the cumulative distribution function), and also fits neatly on the radio/X-ray correlation for a quiescent X-ray binary. In contrast, the three radio/X-ray sources identified in IC 2602 do not fit on the X-ray binary correlation plane at all, but do fit in the Guedel et al. (1995) correlation.

If the radio/X-ray emission from WOCS 3012/S1077 is due to a compact object, and is not of stellar origin, it is more likely to be from a black hole than a neutron star. While neutron stars do sometimes occupy the location on the radio/X-

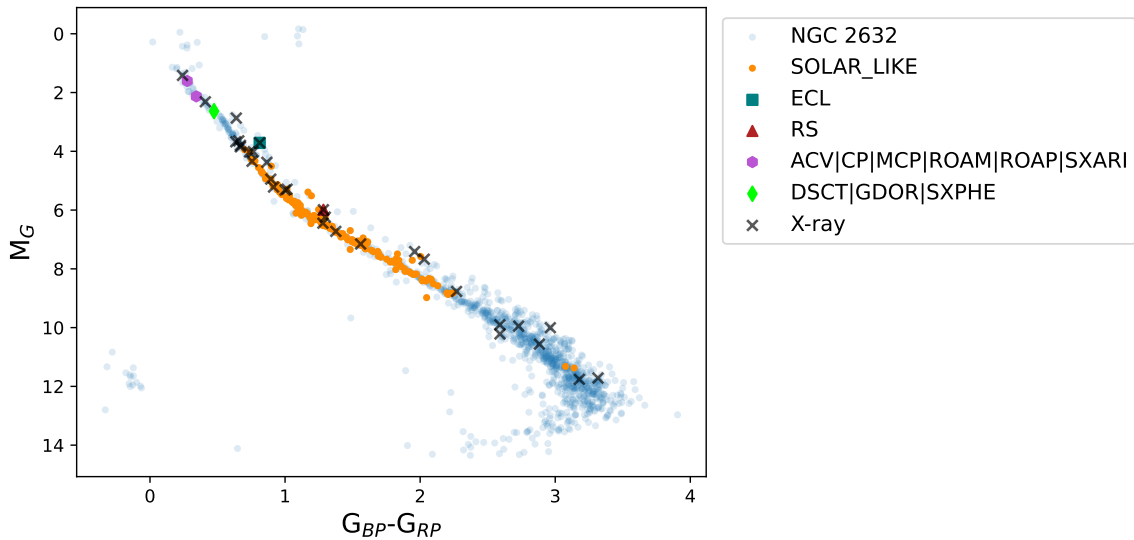


Figure 3. CMD for NGC 2632. Black x's are X-rays from eROSITA, green diamonds are δ Scuti/ γ Doradus/SX Pheonicis, purple pentagons are ACV stars, red triangles are RS Canum Venaticorum, teal squares are eclipsing binaries, and orange points are solar-like variability.

ray correlation generally occupied by black holes, very few neutron stars produce X-ray luminosity this faint (Heinke et al., 2003, 2006; Bahramian et al., 2015; Degenaar et al., 2017; van den Eijnden et al., 2021; Postnov et al., 2022). Because the VLA observation of M67 was only a 4 hour exposure, we also cannot currently rule out that the radio emission is caused by a radio flare star (e.g., Driessen et al., 2024).

Like the putative black hole discovered by Paduano et al. (2024), WOCS 3012/S1077's radio and X-ray emission have ambiguous interpretations, where it falls into both chromospherically active binary stars, and quiescent stellar mass black holes. Spectroscopy by Geller et al. (2021) provides a mass ratio of the inner binary ($q=m_2/m_1$) as 0.76. We assume, based on its location on the CMD, that the inner visible star has just left the main sequence, and the mass is between 1.2 and 1.3 M_{\odot} , suggesting that the unseen secondary has a minimum mass that is roughly solar, but the object's true mass is highly dependent on the inclination angle, which is not constrained. Therefore, this spectroscopic information does not exclude a less luminous star as the unseen companion to the inner binary, and also allows for a neutron star or black hole to explain the system, in the case of a very extreme inclination angle ($> 90\%$).

The long-term X-ray variability, dropping by around two orders of magnitude in X-ray over ~ 15 years may provide a hint as to the nature of the unseen inner binary member. While chromospherically active binaries are known to exhibit X-ray variability (e.g., Kashyap & Drake, 1999; Perdelwitz et al., 2018, among others), a change of two orders of magnitude of X-ray luminosity is highly consistent with behaviors in the accretion processes of black holes and neutron stars (e.g., Tetarenko et al., 2016; Panurach et al., 2021, of many notable examples).

However, the Kepler K2 photometric lightcurve of this source (EPIC 211416111) exhibits optical variability profiles consistent with chromospherically active binaries, with clear

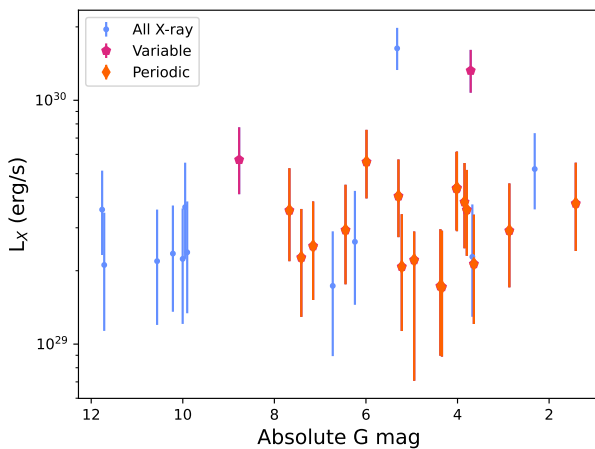


Figure 4. X-ray luminosity (0.5–2.3 keV) versus absolute G magnitude for X-ray sources in NGC 2632. Variable sources are denoted with orange pentagons, and periodic variable sources are marked with pink diamonds.

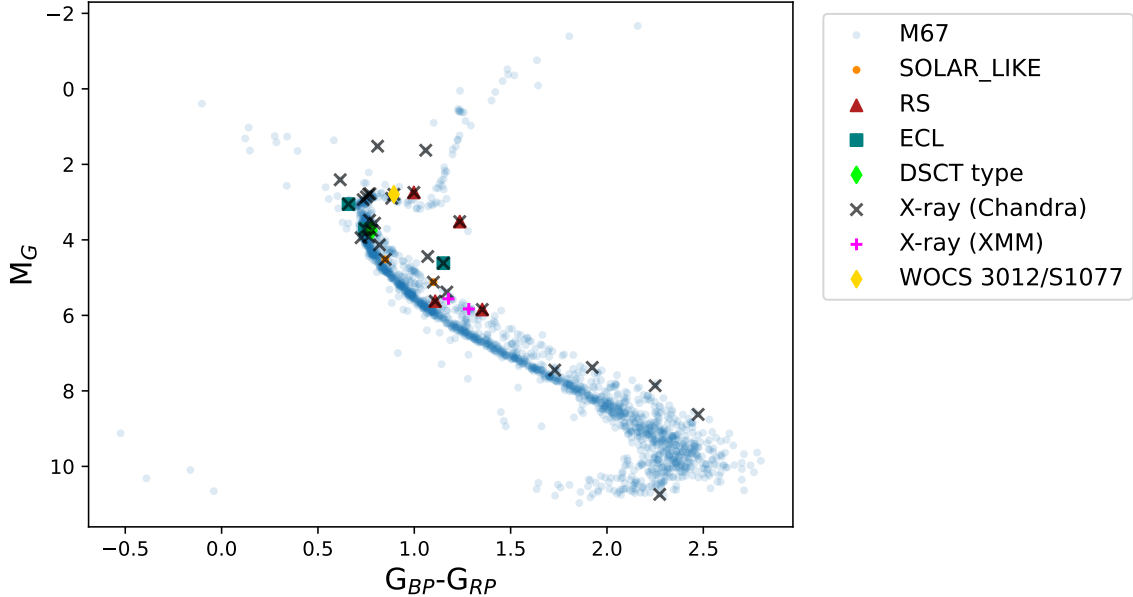


Figure 5. CMD for M67. X-rays from *Chandra* are denoted in x's, and X-rays from XMM-Newton are denoted by purple plusses. Different Gaia variability classifications are shown, a green diamond for pulsating systems δ Scuti/ γ Doradus/SX Pheonicis, teal squares for eclipsing binaries (which are also X-ray sources), red triangles for RS Canum Venaticorum (which are also X-ray sources), and orange dots for solar-like variability.

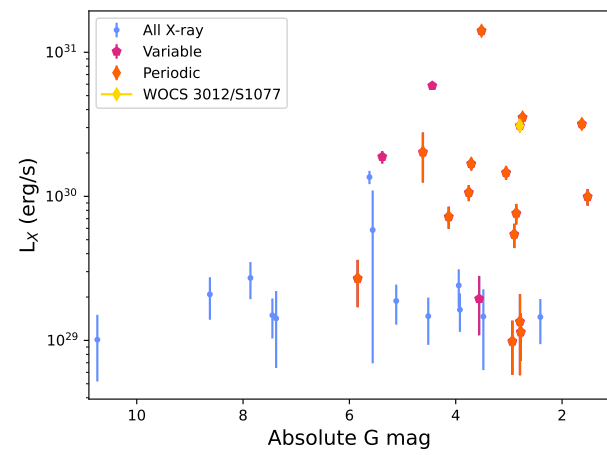


Figure 6. X-ray luminosity (0.5–7.0 keV) versus absolute G magnitude for M67's X-ray sources. Pink diamonds denote periodic variability, while orange pentagons show variability flags from Eyer et al. (2023).

evidence of significant stellar flaring activity. Several optical flares, including a superflare, were identified through visual inspection, all displaying the characteristic flare profile of a rapid rise followed by a relatively slower decay. In addition, notable variations in the lightcurve shape suggest varying starspot activity. Taken together, these findings indicate that this source is likely a chromospherically active binary, rather than a quiescent black hole. However, if the chromospheric activity is coming from a very spun-up primary star at an extreme inclination angle, then it would be possible for this system to also host a quiescent stellar mass black hole.

4. Summary and Conclusions

We take advantage of the wealth of multiwavelength surveys, from X-ray to optical to radio, and we search for multiwavelength contents of three open clusters, IC 2602 (30 Myr), NGC 2632 (0.75 Gyr) and M67 (4 Gyr), using archival X-ray and radio data, and Hunt & Reffert (2024)'s Gaia catalog of cluster members. We identified 77 X-ray sources in IC 2602, many of which were variable systems, and detected evidence of chromospherically active binaries in the EMU survey. In NGC 2632, we found 31 X-ray sources, 27 of which were variable.

NGC 2632 contained the largest number of variable stars (155 stars with solar-like variability). IC 2602 contains a large number of young solar objects, 1 RR Lyrae star, 3 slowly pulsating B stars, and 11 RS Canum Venaticorum. In contrast, M67 contains fewer variable systems, only 21 stars with solar-like variability, and 8 RS Canum Venaticorum stars, with 3 eclipsing binaries, and 1 pulsating DSCT. The X-ray contents of the clusters with known optical variability are presented in Tables 2, 3, and 4, and the overall summary of the optical variability is summarized in Table 6.

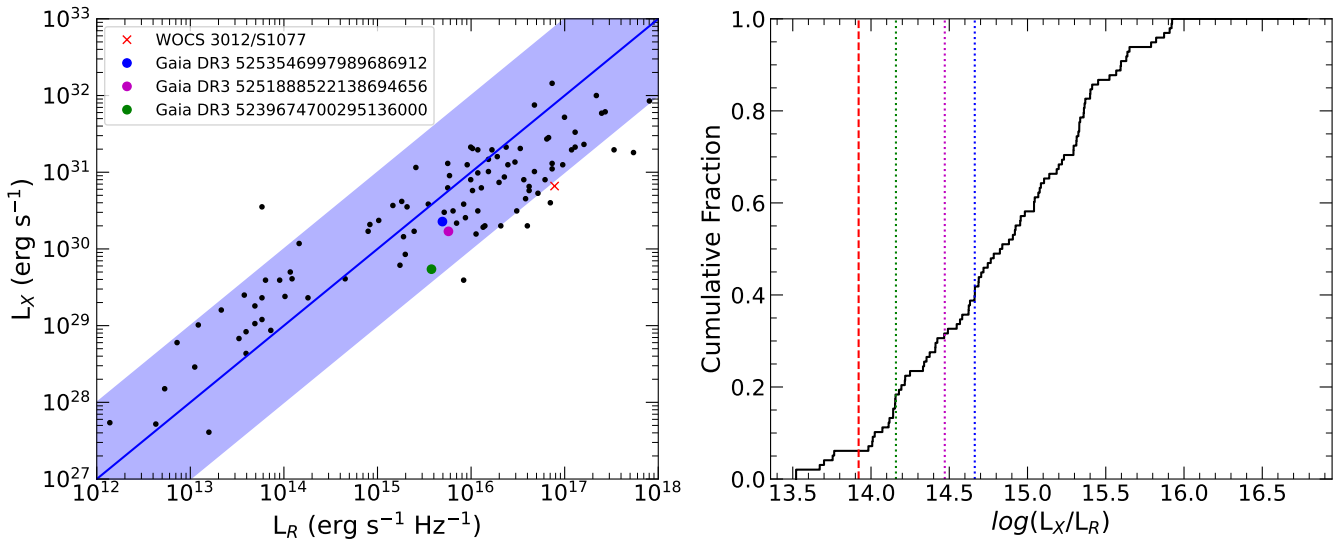


Figure 7. The location of IC 2602 radio/X-ray sources (Table 5) and WOCS 3012/S1077 on the relation of radio and X-ray for active binaries from Guedel et al. (1995). Adapted from Paduano et al. (2024). The three sources in IC 2602 fall firmly on the correlation for active binaries. WOCS 3012/S1077 (dashed line in left hand side) falls in the scatter near the correlation.

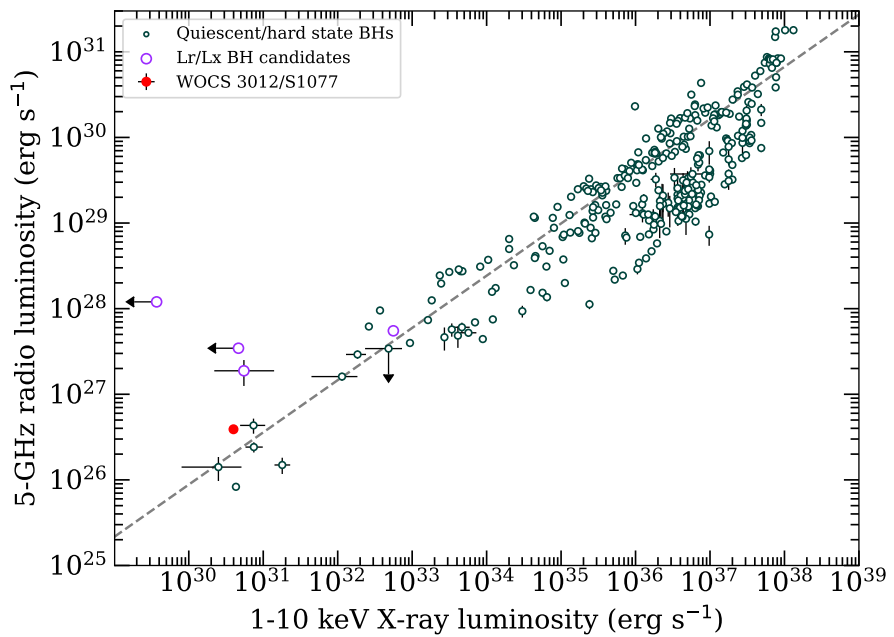


Figure 8. Location of WOCS 3012/S1077 on the radio/X-ray correlation for black holes, next to known quiescent black holes, and black hole candidates. WOCS 3012/S1077 occupies a space on this correlation that is near where one would expect to find a quiescent black hole, based on the X-ray and radio. In comparison, the three X-ray/radio sources identified in IC 2602 are much fainter in X-ray, and several orders of magnitude louder in radio than known X-ray binaries, and are not near the correlation plane at all. Figure modified from Bahramian et al. (2018).

The global study of optical variability in Anderson & Hunt (2025) shows that the fraction of types of variables is dependent on age; young systems like IC 2602 are expected to have a significant number of YSOs. Older systems like NGC 2632 will have a large fraction of solar-like variables, which we also see. At gigayear ages like M67, one expects a rather low fraction of RS systems, however, that is the second highest amount of variable systems seen in M67, highlighting its uniqueness as an old and massive open cluster. Gaia gives us a chance to do a population study of a massive amount of open clusters in the optical, and it is currently unknown how much radio and X-ray flux can be observed as a function of age. With the advent of all sky X-ray and radio surveys, this question can be addressed for the first time. With a larger sample, it may be possible to understand the detailed properties of a cluster's contents by its overall X-ray flux.

M67 may harbor more radio and X-ray sources than the 31 cluster X-ray sources detected, but with the current coverage, we do not yet have a complete picture of its contents, but what we do know is already illuminating.

Modeling dynamical stellar evolution in clusters is one of the most pressing topics in modern astronomy; knowing the behaviors of all individual cluster stellar members is vital for benchmarking simulations of dynamical evolution in star clusters (Hurley & Shara, 2002; Hurley et al., 2007). After around 10 Myr, black holes and neutron stars are expected to start forming in a star cluster system, but their final fates, and if they are retained in the clusters at all are unknown, because their natal kicks are currently not well constrained. Therefore, it is especially interesting to examine these clusters for potential black holes/neutron stars.

This paper demonstrates that by combining modern X-ray and radio surveys, along with new optical cluster studies, it is possible to be sensitive to the high energy emission of compact objects in the very wide variety of open clusters in the Milky Way. Thanks to the wide variety of optical data available on these stars, it is also possible to probe a black hole origin for the high energy emission, as well as capture the broad range of stellar activity in these clusters, which all serve the purpose of better improving models of dynamical evolution in star clusters.

The authors thank the referee for their helpful comments which greatly improved the manuscript. KCD thanks Aaron Geller for helpful discussion, and is indebted to Susmita Sett for her LaTeX skills. This work has made use of data from the European Space Agency (ESA) mission *Gaia* (<https://www.cosmos.esa.int/gaia>), processed by the *Gaia* Data Processing and Analysis Consortium (DPAC, <https://www.cosmos.esa.int/web/gaia/dpac/consortium>). Funding for the DPAC has been provided by national institutions, in particular the institutions participating in the *Gaia* Multilateral Agreement. This work is based on data from eROSITA, the soft X-ray instrument aboard SRG, a joint Russian-German science mission supported by the Russian Space Agency (Roscosmos), in the interests of the Russian Academy of Sciences represented by its Space Research Institute (IKI), and the Deutsches Zentrum für Luft- und Raumfahrt (DLR). The SRG spacecraft

was built by Lavochkin Association (NPOL) and its subcontractors, and is operated by NPOL with support from the Max Planck Institute for Extraterrestrial Physics (MPE). The development and construction of the eROSITA X-ray instrument was led by MPE, with contributions from the Dr. Karl Remeis Observatory Bamberg & ECAP (FAU Erlangen-Nuernberg), the University of Hamburg Observatory, the Leibniz Institute for Astrophysics Potsdam (AIP), and the Institute for Astronomy and Astrophysics of the University of Tübingen, with the support of DLR and the Max Planck Society. The Argelander Institute for Astronomy of the University of Bonn and the Ludwig Maximilians Universität Munich also participated in the science preparation for eROSITA. Facilities: Gaia, XMM-Newton, eROSITA, *Chandra* X-ray Observatory, ASKAP, VLA Software: astropy (Astropy Collaboration et al., 2013), CASA (CASA Team et al., 2022), matplotlib (Hunter, 2007), NumPy (Harris et al., 2020), pandas (McKinney, 2010), LSDB (Caplar et al., 2025)

5. Appendix

We include the crossmatch catalogs of X-ray and optical for IC 2602, NGC 2632 and M67. The X-ray information for IC 2602 and NGC 2632 come from eROSITA, and the X-rays for M67 come from *Chandra*. All three clusters were crossmatched with Gaia, and sub-selected for cluster membership based on Hunt & Reffert (2024). We include eRASS ID, R.A & Dec and positional error from eROSITA, along with the 0.5–2.3 keV flux in erg/s and flux error, and the Gaia ID, R.A. and Dec from optical, along with the maximum match separation. For M67, we include the same information from Gaia and NWAY, and include the *Chandra* positions and fluxes. A preview of these tables is displayed below.

Data Availability Statement All data is publicly available.

References

- Anderson, R. I., & Hunt, E. L. 2025, arXiv e-prints, arXiv:2508.12866
- Astropy Collaboration, Robitaille, T. P., Tollerud, E. J., et al. 2013, A&A, 558, A33
- Bahramian, A., Heinke, C. O., Degenaar, N., et al. 2015, MNRAS, 452, 3475
- Bahramian, A., Miller-Jones, J., Strader, J., et al. 2018, Radio/X-ray correlation database for X-ray binaries, doi:10.5281/zenodo.1252036
- Balbinot, E., Dodd, E., Matsuno, T., et al. 2024, A&A, 687, L3
- Belloni, T., Verbunt, F., & Mathieu, R. D. 1998, A&A, 339, 431
- Boffin, H. M. J., Carraro, G., & Beccari, G., eds. 2015, Astrophysics and Space Science Library, Vol. 413, Ecology of Blue Straggler Stars
- Caillault, J. P. 1996, in ASPCS, Vol. 109, Cool Stars, Stellar Systems, and the Sun, ed. R. Pallavicini & A. K. Dupree, 325
- Cantat-Gaudin, T., & Casamiquela, L. 2024, New Astronomy Reviews, 99, 101696
- Cantat-Gaudin, T., Jordi, C., Vallenari, A., et al. 2018, Astronomy and Astrophysics, 618, A93
- Cantat-Gaudin, T., Anders, F., Castro-Ginard, A., et al. 2020, Astronomy and Astrophysics, 640, A1
- Caplar, N., Beebe, W., Branton, D., et al. 2025, arXiv e-prints, arXiv:2501.02103
- CASA Team, Bean, B., Bhatnagar, S., et al. 2022, PASP, 134, 114501
- Castro-Ginard, A., Jordi, C., Luri, X., et al. 2018, Astronomy and Astrophysics, 618, A59

Gaia DR3 ID	R.A. (Gaia)	Dec (Gaia)	eRASS ID	R.A. (eRASS)	Dec (eRASS)	Err.	Flux	Err.	Sep.
524978364555618432	148.645965	-62.90093	1eRASS J095435.0-625400	148.646036	-62.900183	9.39	6.59E-14	1.98E-14	0.36
5253742607985183872	158.189693	-62.34537	1eRASS J103245.2-622044	158.188495	-62.345570	6.10	3.76E-14	1.26E-14	2.33
5238755920895671040	164.546205	-65.713997	1eRASS J105811.1-654253	164.546500	-65.714733	6.4	1.72E-14	9.26E-15	2.68
5240531632175135616	168.747405	-64.347075	1eRASS J111459.3-642049	168.747367	-64.346954	3.25	2.84E-14	1.02E-14	0.44
5239242660940082432	159.894951	-66.135807	1eRASS J103934.7-660809	159.894713	-66.135931	3.17	5.81E-14	1.42E-14	0.56

GAIA DR3	R.A. (Gaia)	Dec. (Gaia)	<i>Chandra</i> ID	R.A. (Chandra)	Dec. (Chandra)	Flux	Sep.
604906771677660544	133.070113	11.808667	2CXO J085216.8+114831	133.69971	11.8087465	$2.35 \pm 0.9 \text{ E-14}$	0.57
604911307163200000	132.823794	11.741530	2CXO J085117.7+114429	132.823832	11.741510	$2.19 \pm 0.20 \text{ E-14}$	0.15
604911509025877248	132.770062	11.765787	2CXO J085104.8+114556	132.770070	11.765785	$1.23 \pm 0.16 \text{ E-14}$	0.03
604911680824692480	132.797490	11.786319	2CXO J085111.3+114710	132.797398	11.786334	$3.16 \pm 1.09 \text{ E-15}$	0.36
604914983655019520	132.758790	11.817018	2CXO J085102.0+114901	132.758592	11.817090	$2.26 \pm 1.0 \text{ E-15}$	0.75

Cavallo, L., Spina, L., Carraro, G., et al. 2024a, *The Astronomical Journal*, 167, 12

—. 2024b, *AJ*, 167, 12

Degenaar, N., Pinto, C., Miller, J. M., et al. 2017, *MNRAS*, 464, 398

Dias, W. S., Monteiro, H., Moitinho, A., et al. 2021, *Monthly Notices of the Royal Astronomical Society*, 504, 356

Distefano, E., Lanzaflame, A. C., Brugaletta, E., et al. 2023, *A&A*, 674, A20

Donor, J., Frinchaboy, P. M., Cunha, K., et al. 2020, *AJ*, 159, 199

Drake, A. J., Graham, M. J., Djorgovski, S. G., et al. 2014, *ApJS*, 213, 9

Driessen, L. N., Pritchard, J., Murphy, T., et al. 2024, *PASA*, 41, e084

Evans, I. N., Primini, F. A., Glotfelty, K. J., et al. 2010, *ApJS*, 189, 37

Eyer, L., Audard, M., Holl, B., et al. 2023, *A&A*, 674, A13

Fan, X., Burstein, D., Chen, J. S., et al. 1996, *AJ*, 112, 628

Ferraro, F. R., Lanzoni, B., Dalessandro, E., et al. 2012, *Nature*, 492, 393

Gaia Collaboration, Prusti, T., de Bruijne, J. H. J., et al. 2016, *A&A*, 595, A1

Gaia Collaboration, Brown, A. G. A., Vallenari, A., et al. 2018, *A&A*, 616, A1

Gaia Collaboration, Vallenari, A., Brown, A. G. A., et al. 2023, *Astronomy and Astrophysics*, 674, A1

Gaia Collaboration, Panuzzo, P., Mazeh, T., et al. 2024, *A&A*, 686, L2

Geller, A. M., Latham, D. W., & Mathieu, R. D. 2015, *AJ*, 150, 97

Geller, A. M., Mathieu, R. D., Latham, D. W., et al. 2021, *AJ*, 161, 190

Geller, A. M., Leiner, E. M., Bellini, A., et al. 2017, *ApJ*, 840, 66

Guedel, M., Schmitt, J. H. M. M., & Benz, A. O. 1995, *A&A*, 302, 775

Harris, C. R., Millman, K. J., van der Walt, S. J., et al. 2020, *Nature*, 585, 357

Heinke, C. O., Grindlay, J. E., Lugger, P. M., et al. 2003, *ApJ*, 598, 501

Heinke, C. O., Wijnands, R., Cohn, H. N., et al. 2006, *ApJ*, 651, 1098

Heinze, A. N., Tonry, J. L., Denneau, L., et al. 2018, *AJ*, 156, 241

Hopkins, A., Kapinska, A., Marvil, J., et al. 2025, *PASA*, 42, e071

Hunt, E. L., & Reffert, S. 2023, *Astronomy and Astrophysics*, 673, A114

—. 2024, *A&A*, 686, A42

Hunter, J. D. 2007, *Computing In Science & Engineering*, 9, 90

Hurley, J. R., Aarseth, S. J., & Shara, M. M. 2007, *ApJ*, 665, 707

Hurley, J. R., Pols, O. R., Aarseth, S. J., & Tout, C. A. 2005, *MNRAS*, 363, 293

Hurley, J. R., & Shara, M. M. 2002, *ApJ*, 570, 184

Hut, P., McMillan, S., Goodman, J., & et al. 1992, *PASP*, 104, 981

Jansen, F., Lumb, D., Altieri, B., et al. 2001, *A&A*, 365, L1

Jayasinghe, T., Stanek, K. Z., Kochanek, C. S., et al. 2019, *MNRAS*, 486, 1907

Kashyap, V., & Drake, J. J. 1999, *ApJ*, 524, 988

Kraft, R. P., Burrows, D. N., & Nousek, J. A. 1991, *ApJ*, 374, 344

Lacy, M., Baum, S. A., Chandler, C. J., et al. 2020, *PASP*, 132, 035001

Liu, L., & Pang, X. 2019, *The Astrophysical Journal Supplement Series*, 245, 32

McKinney, W. 2010, in *Proceedings of the 9th Python in Science Conference*, ed. S. van der Walt & J. Millman, 51 – 56

Merloni, A., Lamer, G., Liu, T., et al. 2024, *A&A*, 682, A34

Mohan, N., & Rafferty, D. 2015, *PyBDSF: Python Blob Detection and Source Finder*, *Astrophysics Source Code Library*, record ascl:1502.007

Mooley, K. P., & Singh, K. P. 2015, *MNRAS*, 452, 3394

Paduano, A., Bahramian, A., Miller-Jones, J. C. A., et al. 2024, *ApJ*, 961, 54

Palaversa, L., Ivezić, Ž., Eyer, L., et al. 2013, *AJ*, 146, 101

Panurach, T., Strader, J., Bahramian, A., et al. 2021, *ApJ*, 923, 88

Perdelwitz, V., Navarrete, F. H., Zamponi, J., et al. 2018, *A&A*, 616, A161

Perley, R. A., Chandler, C. J., Butler, B. J., & Wrobel, J. M. 2011, *ApJ*, 739, L1

Perren, G. I., Pera, M. S., Navone, H. D., & Vázquez, R. A. 2023, *Monthly Notices of the Royal Astronomical Society*, 526, 4107

Perryman, M. A. C., Lindegren, L., Kovalevsky, J., et al. 1997, *A&A*, 323, L49

Peterson, R. C., Carney, B. W., & Latham, D. W. 1984, *ApJ*, 279, 237

Portegies Zwart, S. F., McMillan, S. L. W., & Gieles, M. 2010, *Annual Review of Astronomy and Astrophysics*, 48, 431

Postnov, K., Kuranov, A., Yungelson, L., & Gil'fanov, M. 2022, in *Astronomy at the Epoch of Multimessenger Studies*, 296–298

Pourbaix, D., Tokovinin, A. A., Batten, A. H., et al. 2004, *A&A*, 424, 727

Rao, K. K., Vaidya, K., Agarwal, M., Balan, S., & Bhattacharya, S. 2023, *MNRAS*, 526, 1057

Reyes, C., Stello, D., Hon, M., et al. 2024, *MNRAS*, 532, 2860

Rivinius, T., Baade, D., & Carciofi, A. C. 2016, *A&A*, 593, A106

Saeedi, S., Liu, T., Knies, J., et al. 2022, *A&A*, 661, A35

Salvato, M., Buchner, J., Budavári, T., et al. 2018, *MNRAS*, 473, 4937

Sandage, A. R. 1953, *AJ*, 58, 61

Shara, M. M., Saffer, R. A., & Livio, M. 1997, *ApJ*, 489, L59

Shi, X.-d., Qian, S.-b., Zhu, L.-y., & Li, L.-j. 2023, *ApJS*, 268, 16

Tetarenko, B. E., Sivakoff, G. R., Heinke, C. O., & Gladstone, J. C. 2016, *ApJS*, 222, 15

Tian, Z., Liu, X., Yuan, H., et al. 2020, *ApJS*, 249, 22

van den Berg, M., Tagliaferri, G., Belloni, T., & Verbunt, F. 2004, *A&A*, 418, 509

van den Eijnden, J., Degenaar, N., Russell, T. D., et al. 2021, *MNRAS*, 507, 3899

Watson, C. L., Henden, A. A., & Price, A. 2006, *Society for Astronomical Sciences Annual Symposium*, 25, 47

Weisskopf, M. C., Brinkman, B., Canizares, C., et al. 2002, *PASP*, 114, 1